

$B_s - \overline{B}_s$ mixing in the MSSM scenario with large flavor mixing in the LL/RR sector

Seungwon Baek¹

Department of Physics, Yonsei University, Seoul 120-749, Korea

Abstract

We show that the recent measurements of $B_s - \overline{B}_s$ mass difference, Δm_s , by DØ and CDF collaborations give very strong constraints on MSSM scenario with large flavor mixing in the LL and/or RR sector of down-type squark mass squared matrix. In particular, the region with large mixing angle and large mass difference between scalar strange and scalar bottom is ruled out by giving too large Δm_s . The allowed region is sensitive to the CP violating phases $\delta_{L(R)}$. The Δm_s constraint is most stringent on the scenario with both LL and RR mixing. We also predict the time-dependent CP asymmetry in $B_s \rightarrow \psi\phi$ decay and semileptonic asymmetry in $B_s \rightarrow \ell X$ decay.

¹sbaek@cskim.yonsei.ac.kr

1 Introduction

The flavor changing processes in the $s - b$ sector are sensitive probe of new physics (NP) beyond the standard model (SM) because they are experimentally the least constrained. In the minimal supersymmetric standard model (MSSM), however, the flavor mixing in the chirality flipping down-type squarks, $\tilde{s}_{L(R)} - \tilde{b}_{L(R)}$, is already strongly constrained by the measurement of $BR(B \rightarrow X_s \gamma)$. On the other hand, large flavor mixing in the chirality conserving $\tilde{s}_{L(R)} - \tilde{b}_{L(R)}$ has been largely allowed. Especially the large mixing scenario in the $\tilde{s}_R - \tilde{b}_R$ sector has been drawing much interest because it is well motivated by the measurement large neutrino mixing and the idea of grand unification [1].

Recently DØ and CDF collaborations at Fermilab Tevatron reported the results on the measurements of $B_s - \overline{B}_s$ mass difference [2, 3]

$$\begin{aligned} 17 \text{ ps}^{-1} < \Delta m_s < 21 \text{ ps}^{-1} \quad (90\% \text{ CL}), \\ \Delta m_s = 17.33^{+0.42}_{-0.21} \pm 0.07 \text{ ps}^{-1}, \end{aligned} \tag{1}$$

respectively. These measured values are consistent with the SM predictions [4, 5]

$$\Delta m_s^{\text{SM}}(\text{UTfit}) = 21.5 \pm 2.6 \text{ ps}^{-1}, \quad \Delta m_s^{\text{SM}}(\text{CKMfit}) = 21.7^{+5.9}_{-4.2} \text{ ps}^{-1} \tag{2}$$

which are obtained from global fits, although the experimental measurements in (1) are slightly lower. The implications of Δm_s measurements have already been considered in model independent approach [6, 7, 8], MSSM models [9, 10], Z' -models [11], *etc.*

In this paper, we consider the implications of (1) on an MSSM scenario with large mixing in the LL and/or RR sector. We do not consider flavor mixing in the LR(RL) sector because they are i) already strongly constrained by $BR(B \rightarrow X_s \gamma)$ [12] and ii) therefore relatively insensitive to $B_s - \overline{B}_s$ mixing. We neglect mixing between the 1st and 2nd generations which are tightly constrained by K meson decays and $K - \overline{K}$ mixing, and mixing between the 1st and 3rd generations which is also known to be small by the measurement of $B_d - \overline{B}_d$ mixing.

The paper is organized as follows. In Section 2, the relevant formulas for $B_s - \overline{B}_s$ mixing are presented. In Section 3 we perform numerical analysis and show the constraints imposed

on our scenario. With these constraints, in Section 4, we predict the time-dependent CP asymmetry in $B_s \rightarrow \psi\phi$ decay and the semileptonic asymmetry in $B_s \rightarrow \ell X$ decay. We conclude in Section 5.

2 $B_s - \overline{B}_s$ mixing in the MSSM scenario with large LL/RR mixing

According to the description of our model in Section 1, the scalar down-type mass squared matrix in the basis where down quark mass matrix is diagonal is given by [13, 14]

$$M_{\tilde{d},LL}^2 = \begin{pmatrix} \tilde{m}_{L11}^{d,2} & 0 & 0 \\ 0 & \tilde{m}_{L22}^{d,2} & \tilde{m}_{L23}^{d,2} \\ 0 & \tilde{m}_{L32}^{d,2} & \tilde{m}_{L33}^{d,2} \end{pmatrix}, \quad M_{\tilde{d},LR(RL)}^2 \equiv 0_{3 \times 3}. \quad (3)$$

The $M_{\tilde{d},RR}^2$ can be obtained from $M_{\tilde{d},LL}^2$ by exchanging $L \leftrightarrow R$. We note that this kind of scenario is orthogonal to the one with flavor violation controlled only by CKM matrix (minimal flavor violation model [15, 8] or the effective SUSY model considered in [16]), where large flavor violation in $s - b$ is impossible a priori.

The mass matrix $M_{\tilde{d},LL}^2$ can be diagonalized by

$$\Gamma_L M_{\tilde{d},LL}^2 \Gamma_L^\dagger = \text{diag}(m_{\tilde{d}_L}^2, m_{\tilde{s}_L}^2, m_{\tilde{b}_L}^2), \quad (4)$$

with

$$\Gamma_L = \begin{pmatrix} 1 & 0 & 0 \\ 0 & \cos \theta_L & \sin \theta_L e^{i\delta_L} \\ 0 & -\sin \theta_L e^{-i\delta_L} & \cos \theta_L \end{pmatrix}. \quad (5)$$

Similarly, the exchange $L \leftrightarrow R$ in (5) gives Γ_R . We restrict $-45^\circ < \theta_{L(R)} < 45^\circ$ so that the mass eigenstate $\tilde{s}(\tilde{b})$ has more strange (beauty) flavor than beauty (strange) flavor.

The most general effective Hamiltonian for $B_s - \overline{B}_s$ mixing

$$H_{\text{eff}} = \sum_{i=1}^5 C_i O_i + \sum_{i=1}^3 \tilde{C}_i \tilde{O}_i \quad (6)$$

has 8 independent operators

$$\begin{aligned}
O_1 &= (\bar{s}_L \gamma_\mu b_L) (\bar{s}_L \gamma^\mu b_L), \\
O_2 &= (\bar{s}_R b_L) (\bar{s}_R b_L), \\
O_3 &= (\bar{s}_R^\alpha b_L^\beta) (\bar{s}_R^\beta b_L^\alpha), \\
O_4 &= (\bar{s}_R b_L) (\bar{s}_L b_R), \\
O_5 &= (\bar{s}_R^\alpha b_L^\beta) (\bar{s}_L^\beta b_R^\alpha), \\
\tilde{O}_{i=1,\dots,3} &= O_{i=1,\dots,3} |_{L \leftrightarrow R}.
\end{aligned} \tag{7}$$

The Wilson coefficients for these $\Delta B = \Delta S = 2$ operators can be obtained by calculating the gluino mediated box diagrams. Since the chargino and neutralino exchanged box diagrams are suppressed by the small gauge coupling constants, we neglect them. In the scenario we are considering, when we consider only LL (RR) mixing, the SUSY box diagram contributes only to C_1 (\tilde{C}_1). When both LL and RR mixing exist simultaneously, there are also contributions to C_4 and C_5 . However, \tilde{C}_2 or \tilde{C}_3 are not generated at all. Note that the induced LR (RL) mixing [17] does not occur, either, because we set $M_{d,LR(RL)}^2 \equiv 0_{3 \times 3}$. Otherwise, the SUSY parameter space is further constrained depending on $\tan \beta$ [17]. The analytic formulas for the Wilson coefficients at the MSSM scale are given by

$$\begin{aligned}
C_1^{\text{MSSM}} &= \frac{\alpha_s^2}{4m_{\tilde{g}}^2} \sin^2 2\theta_L e^{2i\delta_L} \left(f_1(x_{\tilde{b}_L, \tilde{g}}, x_{\tilde{b}_L, \tilde{g}}) - 2f_1(x_{\tilde{s}_L, \tilde{g}}, x_{\tilde{b}_L, \tilde{g}}) + f_1(x_{\tilde{s}_L, \tilde{g}}, x_{\tilde{s}_L, \tilde{g}}) \right), \\
C_{4(5)}^{\text{MSSM}} &= \frac{\alpha_s^2}{4m_{\tilde{g}}^2} \sin 2\theta_L \sin 2\theta_R e^{i(\delta_L + \delta_R)} \left(f_{4(5)}(x_{\tilde{b}_R, \tilde{g}}, x_{\tilde{b}_L, \tilde{g}}) - f_{4(5)}(x_{\tilde{b}_R, \tilde{g}}, x_{\tilde{s}_L, \tilde{g}}) \right. \\
&\quad \left. - f_{4(5)}(x_{\tilde{s}_R, \tilde{g}}, x_{\tilde{b}_L, \tilde{g}}) + f_{4(5)}(x_{\tilde{s}_R, \tilde{g}}, x_{\tilde{s}_L, \tilde{g}}) \right), \\
\tilde{C}_1^{\text{MSSM}} &= C_1^{\text{MSSM}} |_{L \leftrightarrow R},
\end{aligned} \tag{8}$$

where the loop functions are defined as

$$\begin{aligned}
f_1(x, y) &\equiv \frac{1}{9}j(1, x, y) + \frac{11}{36}k(1, x, y), \\
f_4(x, y) &\equiv \frac{7}{3}j(1, x, y) - \frac{1}{3}k(1, x, y), \\
f_5(x, y) &\equiv \frac{1}{9}j(1, x, y) + \frac{5}{9}k(1, x, y),
\end{aligned} \tag{9}$$

and the j and k are defined in [18]. The RG running of the Wilson coefficients down to m_b scale can be found, for example, in [19].

We can calculate the $B_s - \overline{B}_s$ mixing matrix element, which is in the form

$$M_{12}^s = M_{12}^{s,\text{SM}}(1 + R). \quad (10)$$

The mass difference of $B_s - \overline{B}_s$ system is then given by

$$\begin{aligned} \Delta m_s &= 2|M_{12}^s| \\ &= \Delta m_s^{\text{SM}}|1 + R|. \end{aligned} \quad (11)$$

In the SM contribution [20] to the mass matrix element

$$M_{12}^{s,\text{SM}} = \frac{G_F^2 M_W^2}{12\pi^2} M_{B_s} \left(f_{B_s} \hat{B}_{B_s}^{1/2} \right)^2 \eta_B S_0(x_t) (V_{tb} V_{ts}^*)^2, \quad (12)$$

the non-perturbative parameters f_{B_s} and \hat{B}_{B_s} give main contribution to the theoretical uncertainty. Using the combined lattice result [21] from JLQCD [22] and HPQCD [23],

$$f_{B_s} \hat{B}_{B_s}^{1/2} \Big|_{(\text{HP+JL})\text{QCD}} = (0.295 \pm 0.036) \text{ GeV}, \quad (13)$$

the SM predicts

$$\Delta m_s^{\text{SM}} = (22.5 \pm 5.5) \text{ ps}^{-1}, \quad (14)$$

which is consistent with the values in (2) obtained from global fits. For the prediction in (14), we used $\eta_B = 0.551$, $\overline{m}_t^{\overline{MS}}(m_t) = 162.3 \text{ GeV}$ and $V_{ts} = 0.04113$ [24].

Now, inserting the CDF data in (1) and the SM prediction in (14) into (11), we obtain

$$|1 + R| = 0.77_{-0.01}^{+0.02}(\text{exp}) \pm 0.19(\text{th}), \quad (15)$$

where the experimental and theoretical errors were explicitly written. The expression for R in our scenario is given by ²

$$R(\mu_b) = \xi_1(\mu_b) + \tilde{\xi}_1(\mu_b) + \frac{3}{4} \frac{B_4(\mu_b)}{B_1(\mu_b)} \left(\frac{M_{B_s}}{m_b(\mu_b) + m_s(\mu_b)} \right)^2 \xi_4$$

²The \hat{B}_{B_s} in (12) is related to $B_1(\mu_b)$ as [20]

$$\hat{B}_{B_s} \equiv B_1(\mu_b) [\alpha_s^{(5)}(\mu_b)]^{-6/23} \left[1 + \frac{\alpha_s^{(5)}(\mu_b)}{4\pi} J_5 \right]. \quad (16)$$

$$+\frac{1}{4}\frac{B_5(\mu_b)}{B_1(\mu_b)}\left(\frac{M_{B_s}}{m_b(\mu_b)+m_s(\mu_b)}\right)^2\xi_5, \quad (17)$$

where we defined ($i = 1, \dots, 5$)

$$\begin{aligned} \xi_i(\mu_b) &\equiv C_i^{\text{SUSY}}(\mu_b)/C_1^{\text{SM}}(\mu_b), \\ \tilde{\xi}_i(\mu_b) &\equiv \tilde{C}_i^{\text{SUSY}}(\mu_b)/C_1^{\text{SM}}(\mu_b). \end{aligned} \quad (18)$$

The relevant B-parameters are given in [25] by

$$B_1(\mu_b) = 0.86(2) \left(\begin{smallmatrix} +5 \\ -4 \end{smallmatrix}\right), \quad B_4(\mu_b) = 1.17(2) \left(\begin{smallmatrix} +5 \\ -7 \end{smallmatrix}\right), \quad B_5(\mu_b) = 1.94(3) \left(\begin{smallmatrix} +23 \\ -7 \end{smallmatrix}\right). \quad (19)$$

Now we briefly discuss $B \rightarrow X_s \gamma$ constraint. The SUSY parameters we consider are also directly constrained by the measured branching ratio of inclusive radiative B -meson decay, $B \rightarrow X_s \gamma$. We take this constraint into account, although it is not expected to be so severe as in a scenario with LR or RL mixing. In the operator basis given in [26], the SUSY contributions to the Wilson coefficients of magnetic operators in our scenario are

$$\begin{aligned} C_{7\gamma}^{\text{SUSY}} &= -\frac{4}{9}\frac{1}{\lambda_t}\frac{\pi\alpha_s\sin 2\theta_L e^{i\delta_L}}{\sqrt{2}G_F m_g^2}[J_1(x_{b_Lg}) - J_1(x_{s_Lg})], \\ C_{8g}^{\text{SUSY}} &= \frac{1}{\lambda_t}\frac{\pi\alpha_s\sin 2\theta_L e^{i\delta_L}}{\sqrt{2}G_F m_g^2}\left[\left(-\frac{3}{2}I_1(x_{b_Lg}) - \frac{1}{6}J_1(x_{b_Lg})\right) - (b_L \leftrightarrow s_L)\right], \end{aligned} \quad (20)$$

where $\lambda_t = V_{ts}^* V_{tb}$ and

$$\begin{aligned} I_1(x) &= \frac{1 - 6x + 3x^2 + 2x^3 - 6x^2 \log x}{12(1-x)^4}, \\ J_1(x) &= \frac{2 + 3x - 6x^2 + x^3 + 6x \log x}{12(1-x)^4}. \end{aligned} \quad (21)$$

There are also chirality flipped $\tilde{C}_{7\gamma,8g}$ with L replaced by R . Therefore, we can see that in principle $\theta_{L(R)}, \delta_{L(R)}$ and $m_{\tilde{s}} - m_{\tilde{b}}$ can be constrained. Compared to the $LR(RL)$ mixing case where large SUSY contribution $\mathcal{O}(m_{\tilde{g}}/m_b)$ is possible due to the chirality flipping inside the loop, our scenario allows only a small SUSY correction to the SM contributions. In addition, although LL mixing gives a linear correction $\mathcal{O}(C_{7\gamma,8g}^{\text{SUSY}}/C_{7\gamma,8g}^{\text{SM}})$ due to the interference term, RR mixing generates only a quadratic correction $\mathcal{O}(|C_{7\gamma,8g}^{\text{SUSY}}/C_{7\gamma,8g}^{\text{SM}}|^2)$ because it is added incoherently to the SM contribution.

3 Numerical analysis

In this Section, we perform numerical analysis and show the constraints imposed by Δm_s^{exp} . We also consider the $BR(B \rightarrow X_s \gamma)$ constraint.

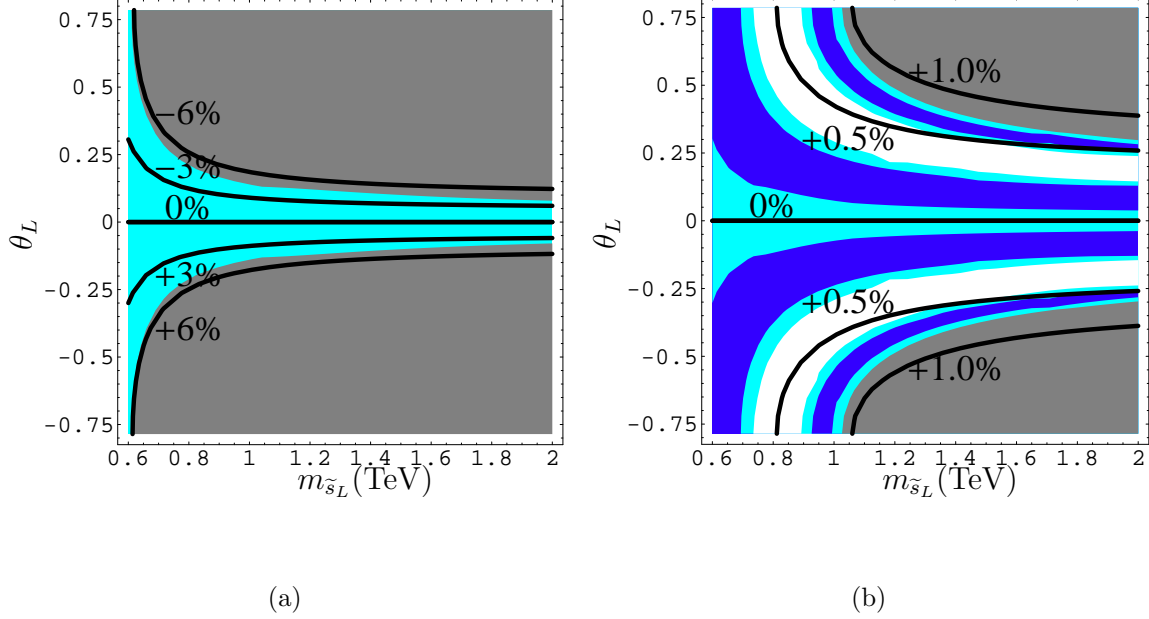


Figure 1: Contour plots for $|1+R|$ in $(m_{\tilde{s}_L}, \theta_L)$ plane. Sky blue region represents 2σ allowed region ($0.39 \leq |1+R| \leq 1.15$), blue 1σ allowed region ($0.58 \leq |1+R| \leq 0.96$), and white (grey) region is excluded at 95% CL by giving too small (large) Δm_s . The labeled thick lines represent the constant $\left(BR^{\text{tot}}(B \rightarrow X_s \gamma) - BR^{\text{SM}}(B \rightarrow X_s \gamma) \right) / BR^{\text{SM}}(B \rightarrow X_s \gamma)$ contours. Only LL mixing is assumed to exist. The fixed parameters are $m_{\tilde{g}} = 0.5$ (TeV), $m_{\tilde{b}_L} = 0.5$ (TeV), (a) $\delta_L = 0$, (b) $\delta_L = \pi/2$.

From (8) it is obvious that the larger the mass splitting between \tilde{s} and \tilde{b} , the larger the SUSY contributions are. Therefore we expect that (15) constrains the mass splitting when the mixing angle $\theta_{L(R)}$ is large. This can be seen in Figure 1 where we show filled contour plots for $|1+R|$ in $(m_{\tilde{s}_L}, \theta_L)$ plane: sky blue region represents 2σ allowed region ($0.39 \leq |1+R| \leq 1.15$), blue 1σ allowed region ($0.58 \leq |1+R| \leq 0.96$), and white (grey) region is excluded at 95% CL by giving too small (large) Δm_s . For these plots we assumed

that only LL mixing exists and fixed $m_{\tilde{g}} = 0.5$ TeV, $m_{\tilde{b}_L} = 0.5$ TeV. In Figure 1(a), we fixed $\delta_L = 0$. We can see that the SUSY interferes with the SM contribution constructively (*i.e.* the SUSY contribution has the same sign with the SM), and when the mixing angle is maximal, *i.e.* $\theta_L = \pm\pi/4$, $m_{\tilde{s}_L} - m_{\tilde{b}_L}$ cannot be greater than about 150 GeV. In Figure 1(b), we set $\delta_L = \pi/2$. The SUSY contribution can interfere destructively (*i.e.* in opposite sign) with the SM and much larger mass splitting is allowed. Therefore we can see that the allowed parameters are sensitive to the CPV phase.

Also the constant $\left(BR^{\text{tot}}(B \rightarrow X_s \gamma) - BR^{\text{SM}}(B \rightarrow X_s \gamma) \right) / BR^{\text{SM}}(B \rightarrow X_s \gamma)$ lines are shown. For fixed θ_L , larger mass splitting $m_{\tilde{s}_L} - m_{\tilde{b}_L}$ gives larger deviation for the branching ratio. This can be understood from (20). However, for very large mass splitting the SUSY contribution decouples and the deviation eventually saturates. We can see that $BR^{\text{tot}}(B \rightarrow X_s \gamma)$ deviates from the SM predictions at most about 5% in the region allowed by Δm_s . Since

$$BR^{\text{exp}}(B \rightarrow X_s \gamma) / BR^{\text{SM}}(B \rightarrow X_s \gamma) = 1.06 \pm 0.13 \quad (22)$$

for $E_\gamma > 1.6$ GeV [27], it is clear that the $BR(B \rightarrow X_s \gamma)$ constraint is completely irrelevant in Figure 1.

The plots for the scenario with RR mixing only are the same with Figure 1 because the expression for $B_s - \bar{B}_s$ is completely symmetric under $L \leftrightarrow R$. As mentioned above, the contribution to $BR(B \rightarrow X_s \gamma)$ is much smaller than LL case.

In Figure 2, contour plots for constant $|1 + R|$ in (θ_L, δ_L) plane are shown. For Figure 2(a)(2(b)), we fixed $m_{\tilde{s}_L} = 0.8(1.0)$ TeV. The other parameters used are the same with those in Figure 1. We can again see the strong dependence on the CPV phase δ_L . It can also be seen that the parameter space with large mixing angle θ_L can be made consistent with the experiments by cancellation with the SM contributions in the destructive interference region (*i.e.* $\delta_L \approx \pi/2$).

Now we consider a scenario with both LL and RR mixing at the same time. Then the operators O_4 and O_5 are additionally generated as mentioned above. They dominate O_1 or \tilde{O}_1 for sizable mixing angles. As a consequence, the constraint on the SUSY parameter

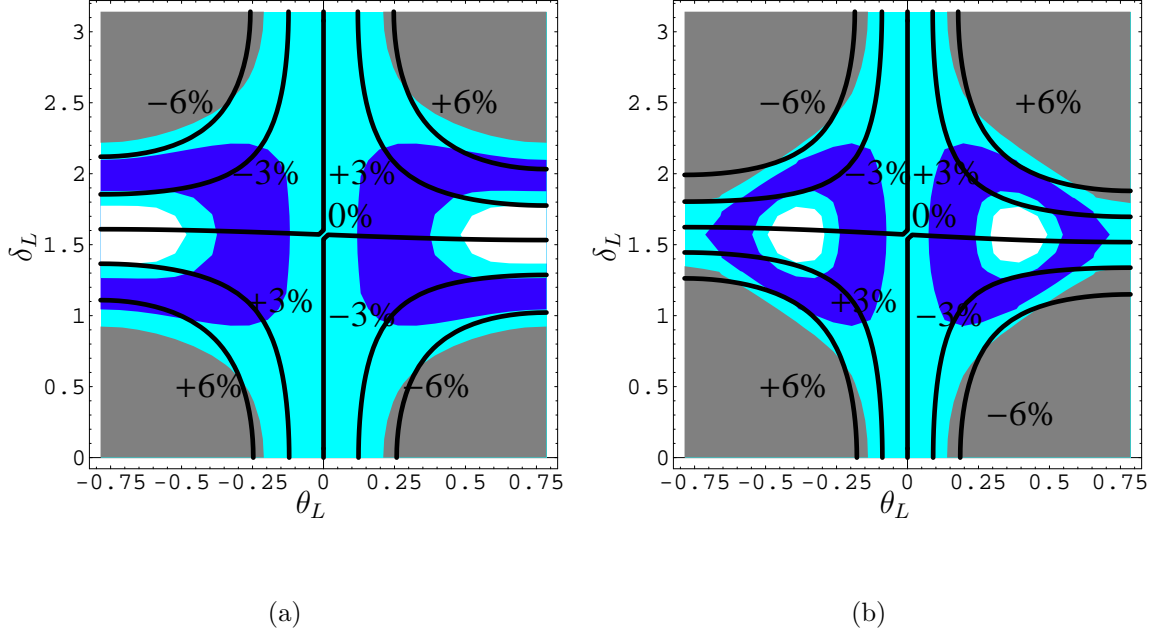


Figure 2: Contour plots for $|1 + R|$ in (θ_L, δ_L) plane. (a) $m_{\tilde{s}_L} = 0.8$ (TeV), (b) $m_{\tilde{s}_L} = 1.0$ (TeV). The rest is the same with Figure 1.

space is very stringent as can be seen in Figure 3. In Figure 3 we set $m_{\tilde{g}} = 0.5$ TeV, $m_{\tilde{b}_L} = m_{\tilde{b}_R} = 0.5$ TeV, $m_{\tilde{s}_L} = m_{\tilde{s}_R} = 0.6$ TeV, and (a) $\delta_L = \delta_R = 0$ (b) $\delta_L = 0, \delta_R = \pi/2$. Even for small mass splitting most region of the parameter space is ruled out by giving too large Δm_s . We can see that $BR(B \rightarrow X_s \gamma)$ is almost insensitive to the change of θ_R as mentioned before.

4 The predictions of $S_{\psi\phi}$ and A_{SL}^s

The CPV phase in the $B_s - \overline{B}_s$ mixing amplitude will be measured at the LHC in the near future through the time-dependent CP asymmetry

$$\frac{\Gamma(\overline{B}_s(t) \rightarrow \psi\phi) - \Gamma(B_s(t) \rightarrow \psi\phi)}{\Gamma(\overline{B}_s(t) \rightarrow \psi\phi) + \Gamma(B_s(t) \rightarrow \psi\phi)} \equiv S_{\psi\phi} \sin(\Delta m_s t). \quad (23)$$

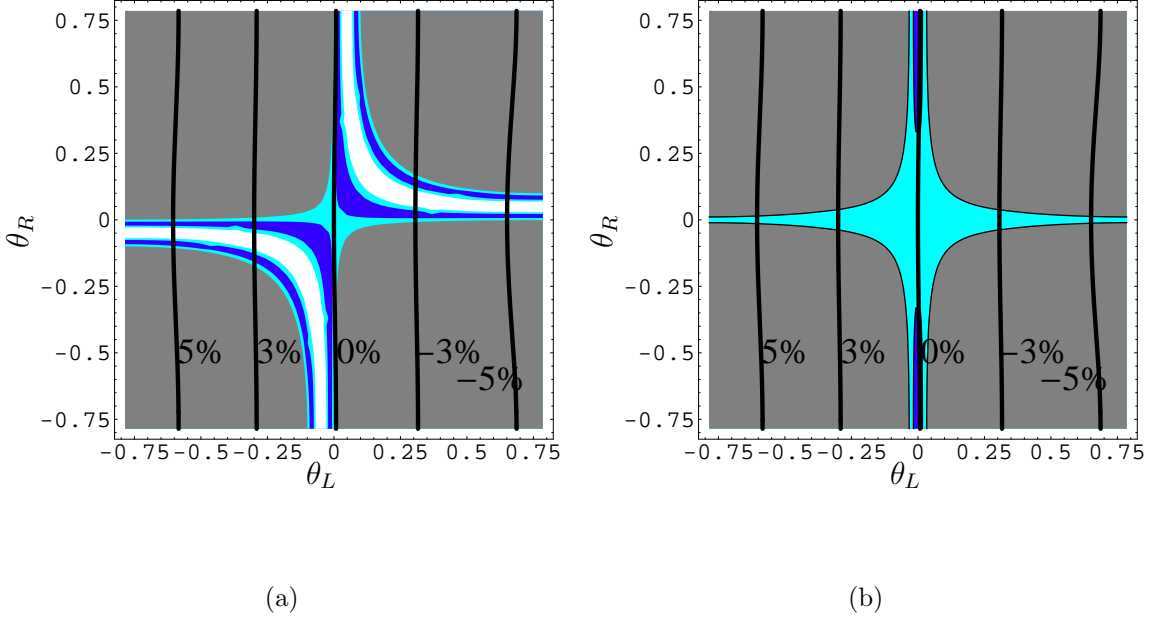


Figure 3: Contour plots for $|1 + R|$ in (θ_L, θ_R) plane. $m_{\tilde{s}_L} = m_{\tilde{s}_R} = 0.6$ (TeV). (a) $\delta_L = \delta_R = 0$ (b) $\delta_L = 0, \delta_R = \pi/2$. We assume both LL and RR mixing exist. The rest is the same with Figure 1.

In the SM, $S_{\psi\phi}$ is predicted to be very small, $S_{\psi\phi}^{\text{SM}} = -\sin 2\beta_s = 0.038 \pm 0.003$ ($\beta_s \equiv \arg[(V_{ts}^* V_{tb})/(V_{cs}^* V_{cb})]$) [7]. If the NP has additional CPV phases, however, the prediction

$$S_{\psi\phi} = -\sin(2\beta_s + \arg(1 + R)) \quad (24)$$

can be significantly different from the SM prediction.

In Figure 4, we show $|1 + R|$ constraint and the prediction of $S_{\psi\phi}$ in $(m_{\tilde{s}_L}, \delta_L)$ plane. However, the $B \rightarrow X_s \gamma$ prediction is not shown from now on because it is irrelevant as mentioned above. For Figure 4(a), we assumed the scenario with LL mixing only and maximal mixing $\theta_L = \pi/4$. We fixed $m_{\tilde{g}} = 0.5$ TeV, $m_{\tilde{b}_L} = 0.5$ TeV. For Figure 4(b), we allowed both LL and RR mixing simultaneously, while fixing $m_{\tilde{g}} = 2$ TeV, $m_{\tilde{b}_L} = m_{\tilde{b}_R} = 1$ TeV, $m_{\tilde{s}_R} = 1.1$ TeV, $\theta_R = \pi/4$, $\delta_L = \pi/4$, and $\delta_R = \pi/2$. In both cases we can see that large $S_{\psi\phi}$ is allowed for large mass splitting between $m_{\tilde{b}_L}$ and $m_{\tilde{s}_L}$. At the moment, $S_{\psi\phi}$ can take any value in the range $[-1, 1]$ even after imposing the current Δm_s^{exp} constraint.

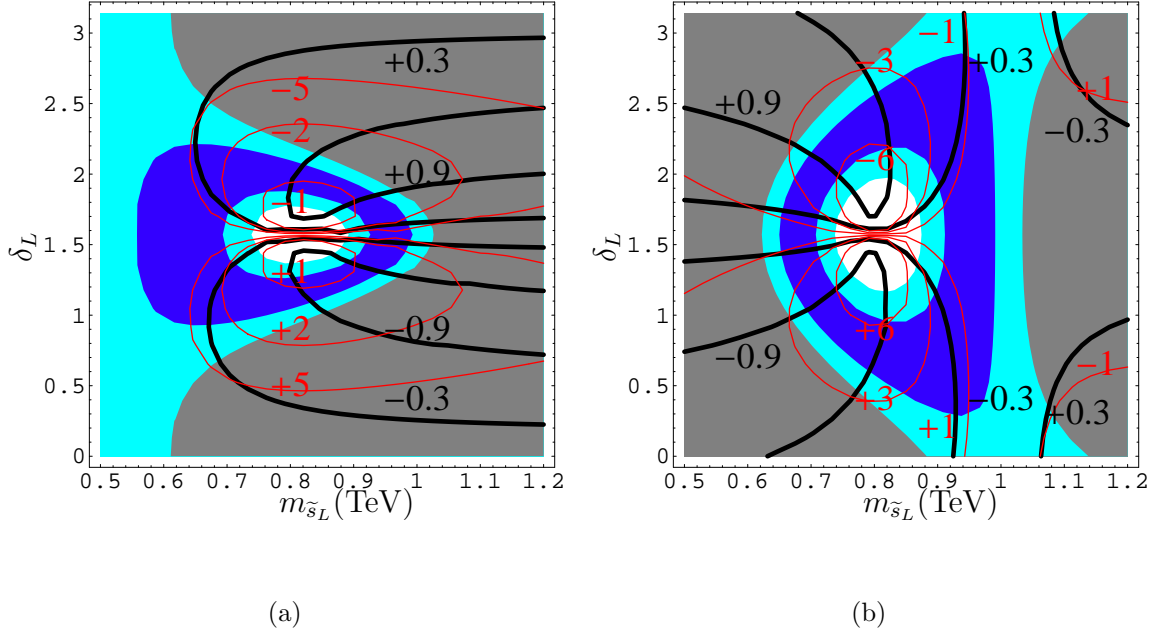


Figure 4: Contour plots for $|1 + R|$ in $(m_{\tilde{s}_L}, \delta_L)$ plane. The $S_{\psi\phi}$ predictions are also shown as thick contour lines. The thin red lines are constant $A_{SL}^s[10^{-3}]$ contours assuming $\text{Re}(\Gamma_{12}^s/M_{12}^s)^{\text{SM}} = -0.0040$. (a) Only LL mixing is assumed to exist. We fixed $m_{\tilde{g}} = m_{\tilde{b}_L} = 0.5$ TeV, $\delta_L = \pi/4$. (b) Both LL and RR mixing are assumed to exist simultaneously. We fixed $m_{\tilde{g}} = 2$ TeV, $m_{\tilde{b}_L} = m_{\tilde{b}_R} = 1$ TeV, $m_{\tilde{s}_R} = 1.1$ TeV, $\theta_R = \pi/4$, $\delta_L = \pi/4$, and $\delta_R = \pi/2$. The rest is the same with Figure 1.

Finally we consider the semileptonic CP asymmetry [28, 16, 7]

$$A_{\text{SL}}^s \equiv \frac{\Gamma(\overline{B}_s \rightarrow \ell^+ X) - \Gamma(B_s \rightarrow \ell^- X)}{\Gamma(\overline{B}_s \rightarrow \ell^+ X) + \Gamma(B_s \rightarrow \ell^- X)} = \text{Im} \left(\frac{\Gamma_{12}^s}{M_{12}^s} \right). \quad (25)$$

It is approximated to be [7]

$$A_{\text{SL}}^s \approx \text{Re} \left(\frac{\Gamma_{12}^s}{M_{12}^s} \right)^{\text{SM}} \text{Im} \left(\frac{1}{1 + R} \right), \quad (26)$$

where $\text{Re}(\Gamma_{12}^s/M_{12}^s)^{\text{SM}} = -0.0040 \pm 0.0016$ [29]. The SM prediction is $A_{\text{SL}}^s(\text{SM}) = (2.1 \pm 0.4) \times 10^{-5}$ [29, 30].

In Figure 4, the thin red lines are constant $A_{SL}^s[10^{-3}]$ contours taking $\text{Re}(\Gamma_{12}^s/M_{12}^s)^{\text{SM}} = -0.0040$. We can readily see that the strong correlation between $S_{\psi\phi}$ and A_{SL}^s . This can

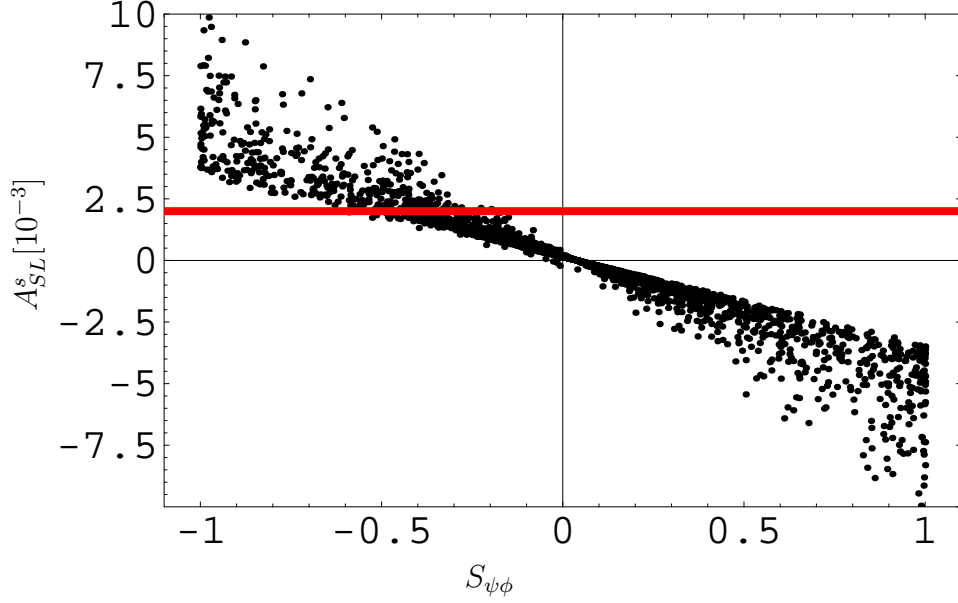


Figure 5: The correlation between A_{SL}^s and $S_{\psi\phi}$. The red line is 1- σ upper bound.

be seen from the relation

$$A_{\text{SL}}^s = - \left| \text{Re} \left(\frac{\Gamma_{12}^s}{M_{12}^s} \right)^{\text{SM}} \right| \frac{S_{\psi\phi}}{|1+R|}. \quad (27)$$

For small R the two observables are linearly correlated as can be seen in Figure 4.

In Figure 5, we show the correlation between A_{SL}^s and $S_{\psi\phi}$. We scanned $0.5 \leq m_{\tilde{g}} \leq 4.0$ TeV, $0.5 < m_{\tilde{b}_L}, m_{\tilde{s}_L} < 2.0$ TeV, $-\pi/4 < \theta_L < \pi/4$ and $0 < \delta_L < 2\pi$, while fixing $m_{\tilde{g}} = m_{\tilde{b}_L} = 0.5$ TeV. The Δm_s constraint is imposed with $0.39 \leq |1+R| \leq 1.15$. We have checked that in the scenario with only LL (RR) mixing, we get the similar correlations. The red line is experimental 1- σ upper bound from $A_{\text{SL}}^s = -0.013 \pm 0.015$ [7]. Now several comments are in order: i) The values for $S_{\psi\phi}$ and A_{SL}^s can be significantly different from the SM predictions. ii) The two observables are strongly correlated. These two facts were already noted in [7]. It has been checked that in the $(\text{Re}R, \text{Im}R)$ plane the above scanned points can completely fill the region allowed by Δm_s . This explains why the correlation in Figure 5 is basically the same with model-independent prediction in [7]. iii) Although it looks like that large negative $S_{\psi\phi}$ value is disfavored, due to large error in $\text{Re}(\Gamma_{12}^s/M_{12}^s)^{\text{SM}}$ we cannot definitely rule out the region at the moment.

5 Conclusions

We considered the MSSM scenario with large LL and/or RR mixing in the down-type mass squared matrix. This scenario is strongly constrained by the recent measurements of $B_s - \overline{B}_s$ mass difference, Δm_s , in contrast with the MSSM scenario where the flavor mixing is controlled only by the CKM matrix [16, 8]. The constraint is most stringent when both LL and RR mixing exist simultaneously. It is also shown that the allowed region is quite sensitive to the CP violating phase.

We also considered the time-dependent CP asymmetry, $S_{\psi\phi}$, and the semileptonic CP asymmetry, A_{SL}^s . It was shown that the $S_{\psi\phi}$ and A_{SL}^s can take values significantly different from the SM predictions. There is also strong correlation between $S_{\psi\phi}$ and A_{SL}^s .

Acknowledgment

The author thanks P. Ko for useful discussions and the organizers of “Workshop on Physics at Hadron Colliders” at KIAS where part of this work was motivated. The work was supported by the Korea Research Foundation Grant funded by the Korean Government (MOEHRD) No. KRF-2005-070-C00030.

References

- [1] S. Baek, T. Goto, Y. Okada and K. i. Okumura, Phys. Rev. D **63**, 051701 (2001) [arXiv:hep-ph/0002141]; S. Baek, T. Goto, Y. Okada and K. i. Okumura, Phys. Rev. D **64**, 095001 (2001) [arXiv:hep-ph/0104146]; D. Chang, A. Masiero and H. Murayama, Phys. Rev. D **67**, 075013 (2003) [arXiv:hep-ph/0205111]; R. Harnik, D. T. Larson, H. Murayama and A. Pierce, Phys. Rev. D **69**, 094024 (2004) [arXiv:hep-ph/0212180].
- [2] V. Abazov [D0 Collaboration], arXiv:hep-ex/0603029.
- [3] G. Gomez-Ceballos [CDF Collaboration], Talk at FPCP 2006, <http://fpcp2006.triumf.ca/agenda.php>.

- [4] M. Bona *et al.* [UTfit Collaboration], JHEP **0603**, 080 (2006) [arXiv:hep-ph/0509219].
- [5] J. Charles *et al.* [CKMfitter Group], Eur. Phys. J. C **41**, 1 (2005) [arXiv:hep-ph/0406184]; <http://ckmfitter.in2p3.fr/>.
- [6] P. Ball and R. Fleischer, arXiv:hep-ph/0604249; A. Datta, arXiv:hep-ph/0605039.
- [7] Z. Ligeti, M. Papucci and G. Perez, arXiv:hep-ph/0604112; Y. Grossman, Y. Nir and G. Raz, arXiv:hep-ph/0605028.
- [8] M. Blanke, A. J. Buras, D. Guadagnoli and C. Tarantino, arXiv:hep-ph/0604057.
- [9] M. Ciuchini and L. Silvestrini, arXiv:hep-ph/0603114; J. Foster, K. i. Okumura and L. Roszkowski, arXiv:hep-ph/0604121; G. Isidori and P. Paradisi, arXiv:hep-ph/0605012. S. Khalil, arXiv:hep-ph/0605021.
- [10] M. Endo and S. Mishima, arXiv:hep-ph/0603251.
- [11] K. Cheung, C. W. Chiang, N. G. Deshpande and J. Jiang, arXiv:hep-ph/0604223.
- [12] F. Gabbiani and A. Masiero, Nucl. Phys. B **322**, 235 (1989); F. Gabbiani, E. Gabrielli, A. Masiero and L. Silvestrini, Nucl. Phys. B **477**, 321 (1996) [arXiv:hep-ph/9604387].
- [13] Y. Grossman, M. Neubert and A. L. Kagan, JHEP **9910**, 029 (1999) [arXiv:hep-ph/9909297];
- [14] S. Baek, D. London, J. Matias and J. Virto, JHEP **0602**, 027 (2006) [arXiv:hep-ph/0511295].
- [15] A. J. Buras, P. Gambino, M. Gorbahn, S. Jager and L. Silvestrini, Phys. Lett. B **500**, 161 (2001) [arXiv:hep-ph/0007085]; G. D'Ambrosio, G. F. Giudice, G. Isidori and A. Strumia, Nucl. Phys. B **645**, 155 (2002) [arXiv:hep-ph/0207036].
- [16] S. Baek and P. Ko, Phys. Rev. Lett. **83**, 488 (1999) [arXiv:hep-ph/9812229]; S. Baek and P. Ko, Phys. Lett. B **462**, 95 (1999) [arXiv:hep-ph/9904283].

- [17] S. Baek, J. H. Jang, P. Ko and J. h. Park, Phys. Rev. D **62**, 117701 (2000) [arXiv:hep-ph/9907572]; S. Baek, J. H. Jang, P. Ko and J. h. Park, Nucl. Phys. B **609**, 442 (2001) [arXiv:hep-ph/0105028].
- [18] G. Colangelo and G. Isidori, JHEP **9809**, 009 (1998) [arXiv:hep-ph/9808487].
- [19] D. Becirevic *et al.*, Nucl. Phys. B **634**, 105 (2002) [arXiv:hep-ph/0112303].
- [20] A. J. Buras, M. Jamin and P. H. Weisz, “LEADING AND NEXT-TO-LEADING QCD CORRECTIONS TO epsilon PARAMETER AND B0 - Nucl. Phys. B **347**, 491 (1990).
- [21] M. Okamoto, “Full determination of the CKM matrix using recent results from lattice PoS **LAT2005**, 013 (2006) [arXiv:hep-lat/0510113].
- [22] S. Aoki *et al.* [JLQCD Collaboration], Phys. Rev. Lett. **91**, 212001 (2003) [arXiv:hep-ph/0307039].
- [23] A. Gray *et al.* [HPQCD Collaboration], Phys. Rev. Lett. **95**, 212001 (2005) [arXiv:hep-lat/0507015].
- [24] J. Charles, arXiv:hep-ph/0606046.
- [25] D. Becirevic, V. Gimenez, G. Martinelli, M. Papinutto and J. Reyes, “B-parameters of the complete set of matrix elements of $\Delta(B) = 2$ JHEP **0204**, 025 (2002) [arXiv:hep-lat/0110091].
- [26] A. L. Kagan and M. Neubert, Eur. Phys. J. C **7**, 5 (1999) [arXiv:hep-ph/9805303].
- [27] The Heavy Flavor Averaging Group (HFAG), <http://www.slac.stanford.edu/xorg/hfag>.
- [28] L. Randall and S. f. Su, Nucl. Phys. B **540**, 37 (1999) [arXiv:hep-ph/9807377].
- [29] M. Beneke, G. Buchalla, A. Lenz and U. Nierste, Phys. Lett. B **576** (2003) 173 [arXiv:hep-ph/0307344].

- [30] M. Ciuchini, E. Franco, V. Lubicz, F. Mescia and C. Tarantino, JHEP **0308** (2003) 031 [arXiv:hep-ph/0308029].